

# Ultrafast Spin Dynamics and Critical Behavior in Half-Metallic Ferromagnet: $\text{Sr}_2\text{FeMoO}_6$

T. Kise,<sup>1</sup> T. Ogasawara,<sup>1</sup> M. Ashida,<sup>2</sup> Y. Tomioka,<sup>3</sup> Y. Tokura,<sup>1,3</sup> and M. Kuwata-Gonokami<sup>1,2,\*</sup>

<sup>1</sup>*Department of Applied Physics, The University of Tokyo, Tokyo 113-8656, Japan*

<sup>2</sup>*Cooperative Excitation Project, ERATO, Japan Science and Technology Corporation (JST), Kanagawa 213-0012, Japan*

<sup>3</sup>*Joint Research Center for Atom Technology (JRCAT), Tsukuba 305-0046, Japan*

(Received 10 March 2000)

Ultrafast spin dynamics in ferromagnetic half-metallic compound  $\text{Sr}_2\text{FeMoO}_6$  is investigated by pump-probe measurements of the magneto-optical Kerr effect. The half-metallic nature of this material gives rise to anomalous thermal insulation between spins and electrons and allows us to pursue the spin dynamics from a few to several hundred picoseconds after the optical excitation. The optically detected magnetization dynamics clearly shows the crossover from microscopic photoinduced demagnetization to macroscopic critical behavior with universal power law divergence of relaxation time for a wide dynamical critical region.

PACS numbers: 75.40.Gb, 71.27.+a, 78.20.Ls, 78.47.+p

Control and manipulation of spins by ultrafast optical excitation, which gives rise to photoinduced magnetization change and magnetic phase transitions in dilute magnetic semiconductor quantum structures [1–3], doped semiconductors [4], and ferromagnetic metals [5–10], have attracted considerable attention. Recent study on the magnetization dynamics in the photoexcited Ni films with nonlinear optical techniques has revealed an ultrafast spin process within 50 fs [9]. Strongly correlated electron systems with a half-metallic nature, which have perfectly spin polarized conducting electrons at the ground state [11], are promising candidates for the study of the photoinduced spin dynamics. These materials possess exotic physical properties such as colossal magnetoresistance, which have strong application potential [12]. The strong coupling between spin, charge, and lattice degrees of freedom in strongly correlated systems makes it possible to manipulate the magnetic properties via cooperative effects induced by optical excitation. In particular, the evidence of photoinduced phase transition accompanied with magnetization changes has been recently reported [13,14]. In order to understand the nature of these phenomena, it is crucial to investigate the temporal evolution of the spin system in the picosecond time scale. Although some attempts have been made by employing pump-probe spectroscopy [15], to the best of our knowledge direct investigation of the ultrafast spin dynamics in half-metallic materials has not been reported so far. Such an investigation can be carried out by exploiting the time resolved magneto-optical Kerr effect (MOKE), which has been shown to be a powerful tool to study the ultrafast dynamics of magnetization [6,16].

We report on the ultrafast pump-probe MOKE and reflectivity study of dynamics of spin and electron systems in the ordered double perovskite  $\text{Sr}_2\text{FeMoO}_6$ , which shows giant magnetoresistance at room temperature [17] and ferromagnetic phase transition with the Curie temperature  $T_C \sim 410\text{--}450\text{ K}$  [18]. Since  $\text{Fe}^{3+}(3d^5; t_{2g}^3 e_g^2, S = 5/2)$  and  $\text{Mo}^{5+}(4d^1; t_{2g}^1, S = 1/2)$  couple antiferromagneti-

cally via exchange interaction and the down-spin electron of  $\text{Mo}^{5+}$  is considered itinerant (upper panel of Fig. 1), a conducting ferrimagnetic ground state with half-metallic nature is expected for this material. The density functional calculation [17] also shows that the occupied up-spin band mainly consists of Fe 3d electrons, while the Fermi level exists within the down-spin band composed of Fe  $t_{2g}$  and Mo  $t_{2g}$  electrons. A large MOKE signal in  $\text{Sr}_2\text{FeMoO}_6$  [19] enables us to investigate the spin dynamics over a wide temporal range from subpicosecond to nanosecond and to obtain the critical exponent of the relaxation time at the magnetic phase transition.

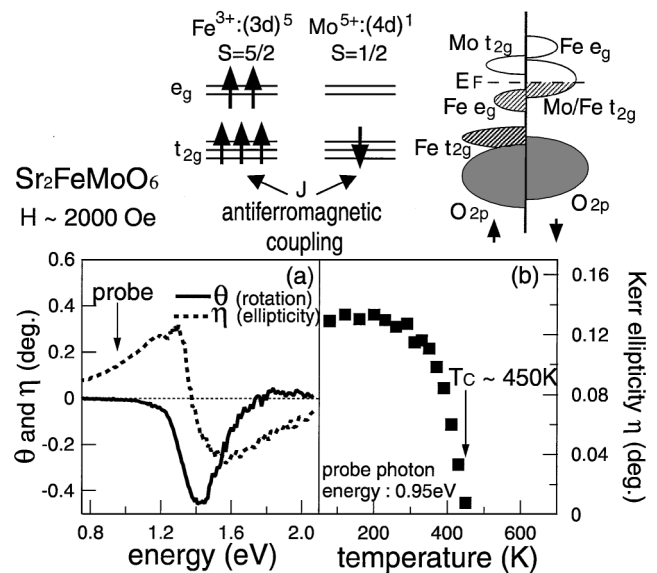


FIG. 1. Magneto-optical Kerr measurements on  $\text{Sr}_2\text{FeMoO}_6$  under the magnetic field of 2000 Oe. (a) Kerr rotation (solid line) and ellipticity (dashed line) spectra at 300 K. (b) Temperature profile of linear Kerr ellipticity probed at 0.95 eV. The upper panel shows the spin configuration of Fe and Mo ions and a schematic of the electronic band structure of  $\text{Sr}_2\text{FeMoO}_6$  based on the density-functional calculations by Kobayashi *et al.* (Ref. [17]).

The MOKE measurements are carried out on single crystal  $\text{Sr}_2\text{FeMoO}_6$ , grown by the floating-zone method [18], in polar Kerr configuration under the magnetic field of 2000 Oe, where the magnetization is nearly saturated at room temperature [17,18]. Figure 1(a) shows the spectral profiles of ellipticity  $\eta$  and rotation angle  $\theta$  at room temperature. We observe the MOKE signal, 1 order of magnitude larger than that of the doped manganites [20]. The MOKE signal is proportional to  $f \cdot M$ , where  $M$  is the magnetization and  $f$  is determined by the complex refractive index at the probe frequency. Correspondingly, the magneto-optical spectra show resonance, known as the plasma enhancement effect [21], around 1 eV, which is close to the plasma edge [18]. The temperature dependence of the  $\eta$ , probed at a photon energy of 0.95 eV, clearly shows the magnetic phase transition at  $T_C = 450$  K [22]. Since the reflectivity is almost temperature independent in this temperature range, the sample magnetization can be monitored with the  $\eta$ .

For the pump-probe measurements, a Ti:sapphire regenerative amplifier system (1 kHz repetition rate) with an optical parametric amplifier (OPA) is used as the light source. The second harmonic of the amplified pulses with a pulse duration of 200 fs, photon energy of 3.1 eV, and a maximum fluence of  $90 \mu\text{J}/\text{cm}^2$  is used as the pump pulse, and its energy is close to the charge transfer excitation from O  $2p$  to Fe/Mo  $t_{2g}$  band with down-spin (see the upper panel in Fig. 1). The probe pulses from the OPA are tuned to 0.95 eV, at which the ellipticity dominates the MOKE signal rather than the rotation effect [Fig. 1(b)]. The pump-probe MOKE measurements are also carried out in polar Kerr configuration and the polarization change of the reflected light from the sample is measured by a balanced detection scheme shown in Fig. 2(a). The photoinduced Kerr ellipticity change  $\Delta\eta_{\text{Kerr}} = \frac{1}{2}[\Delta\eta(M) - \Delta\eta(-M)]$  is measured by changing the sign of the magnetic field in order to eliminate the contribution from the pump induced optical anisotropy. A sensitivity of our measurement system is  $10^{-3}$  deg. The signal is observed to be proportional to the pump beam intensity in all pump-probe measurements.

The inset in Fig. 2(a) shows the transient reflection change  $\Delta R/R$ , measured at 300 K. It shows a sharp reduction in the reflectivity during the pump pulse duration, followed by a fast relaxation within 2–3 ps [region (1)] and a fairly long time plateau up to a few tens of nanoseconds [region (2)]. The reflectivity returns to the initial state in 1 ms by heat diffusion [region (3)]. Figures 2(b) and 2(c) show the  $\Delta R/R$  and ellipticity change  $\Delta\eta_{\text{Kerr}}$  for different temperatures, indicating that the temperature dependence is negligible in  $\Delta R/R$ , while that is significant in  $\Delta\eta_{\text{Kerr}}$ . The temporal evolution of  $\Delta\eta_{\text{Kerr}}$  up to 500 ps is shown in Fig. 3(a) for different temperatures. One can observe that below the Curie point, the ellipticity change can be fitted by  $\Delta\eta_{\text{Kerr}}(t) = \Delta\eta_{\text{step}} + (\Delta\eta_{\text{max}} - \Delta\eta_{\text{step}})(1 - \exp[-t/\tau_{\text{spin}}])$ , where  $\Delta\eta_{\text{step}}$  and  $\Delta\eta_{\text{max}}$  are the instan-

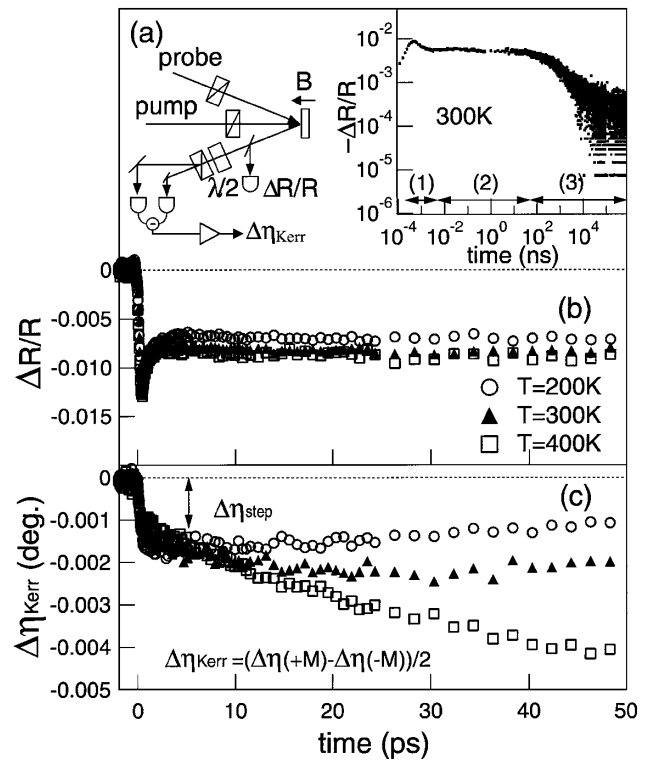


FIG. 2. (a) Schematic of the experimental setup for the pump-probe magneto-optical Kerr measurements. Inset shows the temporal evolution of transient reflection change  $\Delta R/R$  from subpicoseconds up to milliseconds. Temporal evolution of the transient reflection  $\Delta R/R$  (b) and Kerr ellipticity change  $\Delta\eta_{\text{Kerr}}$  (c) up to 50 ps, measured at 200, 300, and 400 K.

taneous decrease and quasiequilibrium value of  $\Delta\eta_{\text{Kerr}}$ , respectively.  $-\Delta\eta_{\text{max}}$ , which shows linear dependence on the pump intensity, increases drastically close to  $T_C$  as shown in Fig. 3(b).

The most striking feature is the very slow spin thermalization observed in the  $\Delta\eta_{\text{Kerr}}$  signal in comparison with the electron thermalization observed in transient  $\Delta R/R$  data. The electron temperature rises rapidly by the optical excitation and it relaxes within 2–3 ps to reach quasiequilibrium temperature, which is 8–10 K, higher than the initial temperature. The fast decay of transient reflectivity indicates that the local heat transfer from electron to the lattice system is completed within a few picoseconds, accompanied by the lattice heat-up. Similar behavior of the electron system is observed in Ni [6]. On the other hand, the behavior of the spin system in  $\text{Sr}_2\text{FeMoO}_6$  is very different. Specifically, the very slow spin thermalization [see Fig. 2(c)], which is pronounced at higher temperature, indicates the anomalously small heat exchange between electrons and spins in  $\text{Sr}_2\text{FeMoO}_6$ . Such an electron-spin thermal insulation can be attributed to the half-metallic electronic structure where conducting electrons are perfectly spin polarized in the down-spin band and isolated from the insulating up-spin band (see the upper panel in Fig. 1). Thermal motion of electrons around the Fermi

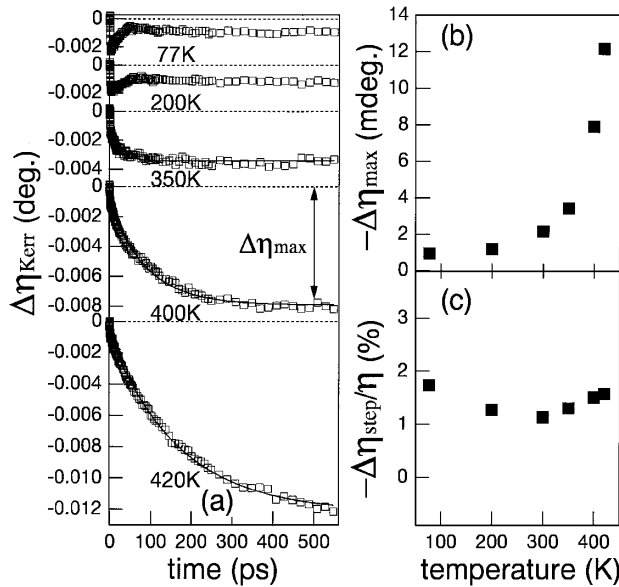


FIG. 3. (a) Temporal evolution of photoinduced Kerr ellipticity  $\Delta\eta_{\text{Kerr}}$  up to 500 ps, measured at various temperatures. Solid lines are the exponential fit. Temperature profiles of  $\Delta\eta_{\text{max}}$  (b) and rapid component  $\Delta\eta_{\text{step}}$  normalized to linear Kerr ellipticity  $\eta$  (c).

level in the spin polarized conduction band does not increase the spin temperature.

From the observed results, we have the following scenario for the temporal evolution of electron, lattice, and spin systems in  $\text{Sr}_2\text{FeMoO}_6$ . Initially, during the photoexcitation ( $\leq 1$  ps), the electron system is heated up and rapidly thermalized due to electron-electron interaction. In this first stage the ellipticity shows a sharp decrease ( $\Delta\eta_{\text{step}}$ ). In the next stage, the electron system relaxes by its energy transfer to the lattice system. The electron and lattice systems reach the quasiequilibrium state ( $\sim 5$  ps) by the electron-phonon interaction, leaving the spin system at its initial temperature. After that, the spin slowly relaxes toward this quasiequilibrium state through weak heat exchange with the reservoir at quasiequilibrium temperature. Finally, the system returns to the initial state by heat diffusion.

The sharp decrease in the ellipticity is the major feature of the initial stage [see Fig. 2(c)]. Since the MOKE signal is proportional to  $f \cdot M$ , both the photoinduced change in the refractive index ( $\Delta f/f \sim \Delta R/R$ ) as well as the photoinduced magnetization change ( $\Delta M/M$ ) contribute to  $\Delta\eta_{\text{step}}/\eta$ , which shows a weak temperature dependence [see Fig. 3(c)]. Though the relative instantaneous changes in the ellipticity and reflectivity are of the same order,  $\Delta\eta_{\text{step}}/\eta \sim \Delta R/R \sim 0.01$ , the subsequent temporal evolution of  $\Delta\eta_{\text{Kerr}}$  in the picosecond time scale is very different from that of  $\Delta R$ . This indicates the direct demagnetization by resonant optical excitation. However, as has been discussed in recent papers on Ni [6–9], it is premature to directly connect the MOKE signal with demagnetization in such an ultrafast time scale.

We now discuss the temporal evolution of the MOKE signal in the second stage, when the electron and lattice system have reached the quasiequilibrium [plateau region (2) in the inset in Fig. 2(a)]. The dramatic increase in  $\Delta\eta_{\text{max}}$  [see Fig. 3(b)] and the relaxation time  $\tau_{\text{spin}}$  as the temperature approaches  $T_C$  indicates that the time resolved signal directly reflects the critical behavior of magnetic phase transition. The spin temperature at the quasiequilibrium, which can be estimated from Fig. 3(b) and the temperature dependence of the  $\eta$  [Fig. 1(a)], is in good agreement with the electron temperature estimated from  $\Delta R/R$ .

The time resolved MOKE measurements give us a unique opportunity to study the dynamics of a spin system independently from other degrees of freedom and obtain the critical characteristics of the ferromagnetic phase transition. The dynamics of the second order phase transition can be described by the dynamical scaling theory [23–25], which allows us to relate the critical behavior of the kinetic parameters (e.g., relaxation time) to the critical exponents of the static parameters (e.g., correlation length) on both sides of the critical point. The theory predicts that in the vicinity of  $T_C$ , the relaxation time behaves as  $\tau \propto |T - T_C|^{-z\nu}$ , where  $\nu$  and  $z$  denote the critical exponent of the correlation length and the dynamical critical exponent, respectively. Figure 4 shows the temperature dependence of  $\tau_{\text{spin}}$  as a function of  $|T' - T_C|$ , where  $T'$  denotes the quasiequilibrium temperature at the region (2) in the inset in Fig. 2(a). One can observe the power law divergence with  $z\nu = 1.22 \pm 0.06$  for the spin relaxation time in the vicinity of  $T_C$  [26]. It should be emphasized that the power law behavior is established in the time scale of a few tens of picoseconds, while the dynamical critical region is much wider than for conventional metals [27].

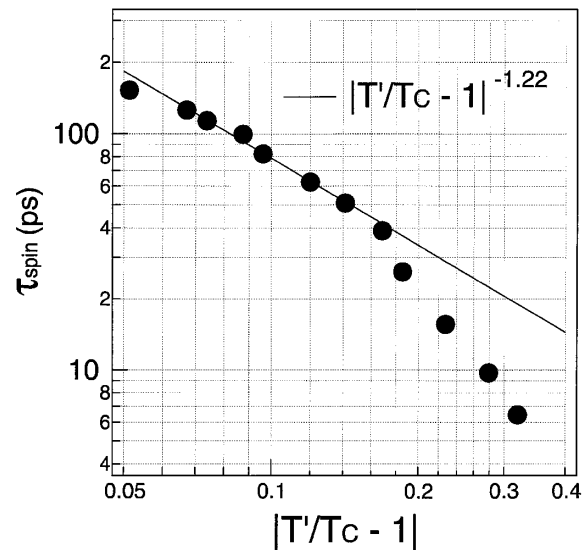


FIG. 4. Temperature dependence of spin relaxation time  $\tau_{\text{spin}}$  as a function of  $|T' - T_C|$ . The solid line is a power law fit  $|T'/T_C - 1|^{-z\nu}$  for the points near  $T_C$ . The fit returns  $z\nu = 1.22 \pm 0.06$ .

Since 3D Ising and Heisenberg models predict  $z\nu \approx 1.30$  [28] and 1.37 [29], respectively, while the 2D Ising model gives  $z\nu \approx 2.165$  [30], our measurements clearly indicate three dimensionality of the spin system in  $\text{Sr}_2\text{FeMoO}_6$ .

We have presented ultrafast spin dynamics in the ordered double perovskite  $\text{Sr}_2\text{FeMoO}_6$  by using the time resolved MOKE technique. We have observed, for the first time, extremely slow relaxation of spins, thermally insulated from electron and lattice systems due to the half-metal nature of this material. The thermal insulation of a spin system provides us a unique opportunity to examine the nonequilibrium spin dynamics near the critical point in a time scale from the picosecond to the nanosecond range. We clearly demonstrate crossover from ultrafast microscopic spin relaxation to macroscopic critical behavior. In the vicinity of the critical point, the spin relaxation time increases as  $|T - T_C|^{-(1.22 \pm 0.06)}$ , which is consistent with the theoretical prediction for the 3D ferromagnetic system. A very fast decrease in the MOKE signal caused by charge transfer optical excitation suggests the direct photoinduced process of the spin system, although the underlying physical mechanism is not established yet.

The authors are grateful to S. Miyashita, N. Ito, N. Nagaosa, M. Ueda, Yu. P. Svirko, and C. Ramkumar for illuminating discussions. This work is supported in part by a grant-in-aid for COE Research from the Ministry of Education, Science, Sports and Culture of Japan and the New Energy and Industrial Technology Development Organization (NEDO).

---

\*Author to whom correspondence should be addressed.

Electronic address: gonokami@ap.t.u-tokyo.ac.jp

- [1] C. Buss *et al.*, Phys. Rev. Lett. **78**, 4123 (1997); M. Haddad *et al.*, Appl. Phys. Lett. **73**, 1940 (1998).
- [2] S. A. Crooker *et al.*, Phys. Rev. B **56**, 7574 (1997).
- [3] J. J. Baumberg *et al.*, Phys. Rev. B **50**, 7689 (1994).
- [4] J. M. Kikkawa and D. D. Awschalom, Phys. Rev. Lett. **80**, 4313 (1998); Nature (London) **397**, 139 (1999); Science **287**, 473 (2000).
- [5] A. Vaterlaus, T. Beutler, and F. Meier, Phys. Rev. Lett. **67**, 3314 (1991).
- [6] E. Beaurepaire, J.-C. Merle, A. Daunois, and J.-Y. Bigot, Phys. Rev. Lett. **76**, 4250 (1996).
- [7] J. Hohlfeld, E. Matthias, R. Knorren, and K. H. Bennemann, Phys. Rev. Lett. **78**, 4861 (1997).
- [8] A. Scholl, L. Baumgarten, R. Jacquemin, and W. Eberhardt, Phys. Rev. Lett. **79**, 5146 (1997).
- [9] J. Gudde *et al.*, Phys. Rev. B **59**, R6608 (1999).
- [10] E. Beaurepaire *et al.*, Phys. Rev. B **58**, 12 134 (1998).
- [11] J.-H. Park *et al.*, Nature (London) **392**, 794 (1998).
- [12] For a review, see *Colossal Magnetoresistive Oxides*, edited by Y. Tokura (Gordon & Breach Publishers, New York, 2000).
- [13] K. Miyano, T. Tanaka, Y. Tomioka, and Y. Tokura, Phys. Rev. Lett. **78**, 4257 (1997).
- [14] Y. G. Zhao *et al.*, Phys. Rev. Lett. **81**, 1310 (1998).
- [15] K. Matsuda, A. Machida, Y. Moritomo, and A. Nakamura, Phys. Rev. B **58**, R4203 (1998).
- [16] Ganping Ju *et al.*, Phys. Rev. Lett. **82**, 3705 (1999).
- [17] K.-I. Kobayashi *et al.*, Nature (London) **395**, 677 (1998).
- [18] Y. Tomioka *et al.*, Phys. Rev. B **61**, 422 (2000).
- [19] K. Shono, M. Abe, M. Gomi, and S. Nomura, Jpn. J. Appl. Phys. **20**, L426 (1981).
- [20] S. Yamaguchi, Y. Okimoto, K. Ishibashi, and Y. Tokura, Phys. Rev. B **58**, 6862 (1998).
- [21] H. Feil and C. Haas, Phys. Rev. Lett. **58**, 65 (1987).
- [22] The slight deviation of  $T_C$  from the results of Ref. [18] may be due to the improved site order of Fe and Mo, which is sensitive to the sample preparation and annealing temperature.
- [23] M. E. Fisher and M. N. Barber, Phys. Rev. Lett. **28**, 1516 (1972); M. N. Barber, in *Phase Transition and Critical Phenomena*, edited by C. Domb and J. L. Lebowitz (Academic Press, London, 1983), Vol. 8.
- [24] M. Suzuki, Phys. Lett. **58A**, 435 (1976); Prog. Theor. Phys. **58**, 1142 (1977).
- [25] S. Miyashita and H. Takano, Prog. Theor. Phys. **73**, 1122 (1985).
- [26] In the close vicinity of the critical point the system is very sensitive to external fields and the possible thermal drift effects would be pronounced. Correspondingly, in order to minimize the possible uncertainty in the estimation of the critical exponent, we intentionally avoid the experimental point closest to  $T_C$  in Fig. 4 for fitting.
- [27] K. Huang, in *Statistical Mechanics* (John Wiley & Sons, New York, 1987), 2nd ed., p. 437.
- [28] N. Ito, Physica (Amsterdam) **192A**, 604 (1993).
- [29] P. Peszak and D. P. Landau, J. Appl. Phys. **67**, 5427 (1990).
- [30] N. Ito, Physica (Amsterdam) **194A**, 591 (1993).